

FREQUENCY STABILIZATION OF A cw DYE LASER AND  
LASER SATURATION OF ATOMIC BEAMS\*

R. L. Barger, T. C. English, J. B. West  
Time and Frequency Division  
National Bureau of Standards  
Boulder, Colorado 80302

Summary

Techniques are described which allow the frequency of a tunable, cw dye laser to be stabilized to 1.5 kHz for integration times up to  $10^{-1}$  sec, 3 kHz at 1 sec, and 300 Hz at 300 sec. Using these techniques, the laser can be tuned to any desired frequency and then stabilized with a long term stability approaching that of a methane-stabilized laser.

Experiments are presently in progress which will use this laser to study saturated absorption of magnetically deflected atomic beams of elements having long-lived excited states. This work may lead to desirable wavelength/frequency standards in the visible region of the optical spectrum. A promising candidate is the  $^1S_0 - ^3P_1$  intercombination transition (6573 Å) of calcium which has a lifetime-limited Q of about  $10^{12}$ .

The dye laser is also being used for an accurate measurement of the Balmer  $\alpha$ ,  $n = 2$  to  $n = 3$  transition (6563 Å) in a beam of metastable hydrogen atoms. This experiment should allow a determination of the Rydberg constant to an accuracy of several parts in  $10^{10}$ .

Dye Laser Stabilization

Previously, stabilized cw dye lasers<sup>1,2</sup> have exhibited either poor long term stability or restricted tuning capability. The method described here provides greatly improved short term frequency stability, virtually no long term drift, and yet allows retention of the full tuning flexibility of the laser.

Dye Laser

The dye laser uses a dye jet, an astigmatically compensated cavity, and a birefringent quartz wavelength selector for coarse tuning. Two intracavity etalons restrict the laser oscillation to a single longitudinal mode. Proper adjustment of the end mirrors on the cavity ensures operation in the lowest order ( $TEM_{00}$ ) transverse mode. The dye (cresyl-violet) is pumped using an off-axis beam from a broadband dye jet laser ( $\lambda \approx 6000$  Å) which, in turn, is pumped by the visible radiation from an argon ion laser. The advantage of using the intermediate

(broadband) laser is that cresyl-violet absorbs more efficiently in the yellow than in the blue and green, and the overall efficiency is thereby increased (even allowing for the ~20% efficiency in converting the blue and green to yellow).

Frequency Stabilization Method

Since a detailed description of the frequency stabilization scheme has been given elsewhere,<sup>3</sup> only the essential features will be described here.

The frequency stabilization system is shown in Fig. 1. The visible output (wavy line) of the stabilized laser is passed through a high finesse Fabry-Perot (FP) servo cavity. The transmitted intensity on the side of the FP fringe is monitored by a fast photodiode. Assume, for purposes of discussion, that the length of the servo cavity remains constant, and also that the intensity of the laser beam at the output mirror of the laser does not change. Should the frequency of the dye laser change, there will be a spatial shift of the FP fringe and, consequently, a change in the intensity of the transmitted light through the servo cavity, as monitored by the photodiode. This change in intensity can be used to provide an error signal for a servo system. After initial wideband amplification, this error signal is split into two parts. The first is a slow part which is applied as a correction voltage to a piezoelectric transducer (PZT) upon which is mounted the output mirror of the stabilized laser. This slow error signal serves to change the length of the laser cavity so as to compensate for slow changes in the laser frequency. The second portion of the error signal is a fast part which is applied to a deuterated KDP (KD\*P) crystal. This fast correction voltage produces changes in the crystal's index of refraction. Since the KD\*P crystal is located inside the cavity of the stabilized dye laser, the applied correction voltage, in effect, changes the optical path length of the cavity, thereby compensating for fast frequency fluctuations.

Amplitude fluctuations of the laser output are prevented from mapping into the frequency domain by using a differential detection scheme (not shown) to monitor the FP fringe. In addition, the laser is intensity stabilized to about one part in  $10^4$  using an external ADP crystal and a separate servo system (neither of which are shown in Fig. 1.).

The high finesse servo cavity is constructed

\*Contribution of the National Bureau of Standards - not subject to copyright.

from a solid quartz rod,  $7\frac{1}{2}$  cm in diameter and 18 cm in length. A small bore in the center allows the light to pass through. The cavity is formed using a mirror at each end of the rod. This method of construction of the servo cavity reduces length variations arising from vibrations and rapid temperature changes, thereby contributing to the short-term frequency stabilization of the dye laser.

To achieve good long-term frequency stability of the laser, the length of the servo cavity is locked to the  $3.39\ \mu\text{m}$  output of He-Ne local oscillator laser. The frequency of the local oscillator is stabilized by offset locking it to a methane stabilized He-Ne laser using standard techniques.<sup>4</sup> The output of the local oscillator (small circles in Fig. 1) is passed through the servo cavity simultaneously with the visible dye laser output. (The dashed mirrors in Fig. 1 are partially reflecting in the visible, and transmitting in the infrared.) The  $3.39\ \mu\text{m}$  fringe signal is detected by an IR photodiode, and the resultant error signal is applied to the servo cavity PZT (cross hatched in Fig. 1). This scheme serves to lock the length of the servo cavity to the methane-stabilized laser.

### Tunability

The frequency of the dye laser can be varied in any one of three ways.

(1) Manual tuning (rotation) of the birefringent filter allows tuning of the laser over the gain curve of the dye. Adjustment of the intracavity etalons provides finer tuning.

(2) The dye laser and servo cavity are enclosed in a pressurized box. By varying the pressure, the servo stabilized laser output can be tuned over a range of about  $2\text{\AA}$ .

(3) The length of the servo cavity can be changed by varying the offset lock of the He-Ne local oscillator. The local oscillator can be tuned  $\pm 220\ \text{MHz}$  from the center of the He-Ne gain curve. This allows electrical tuning of the dye laser over a range of 2.5 GHz.

The method used to stabilize the dye laser at a desired frequency is to coarse tune it using pressure tuning. This can be done while the dye laser is locked to the servo cavity, but the servo cavity is not locked to the methane-stabilized laser. When the laser is approximately tuned to the desired frequency, the servo cavity is locked to the He-Ne local oscillator. The dye laser can then be electrically tuned over a 2.5 GHz range while in the fully locked and stabilized condition.

### Power Output

Approximately 5 W of  $\text{Ar}^+$  all-line  $\text{TEM}_{00}$  power produces in excess of 1 W cw at  $6000\ \text{\AA}$  when rhodamine 6G is used in the broadband dye laser. When this radiation is used to pump the stabilized laser, 8 mW can be obtained at  $6600\ \text{\AA}$  with the laser in the fully locked condition. Modifications are now in progress to allow pumping of the broadband laser using two  $\text{Ar}^+$  lasers, each with  $> 5\ \text{W}$  output.

This should allow a significant increase in the output power of the stabilized laser since the latter is presently operating close to threshold.

### Frequency Stability

The dye laser frequency stability was measured by observing signals in a separate, high finesse, Fabry-Perot analyzing cavity. This analyzing cavity was nearly identical to the servo cavity. The signal was amplified with gain flat to 5 MHz and processed by a voltage-to-frequency converter and computing counter. Figure 2 is a plot of the resulting Allan variance,  $\sigma$ , as a function of averaging time,  $\tau$ . In obtaining the frequency stability data, rhodamine 6G was used in the stabilized dye laser. However, it is not expected that the stability using cresyl-violet will be significantly different.

Curve A in Fig. 2 shows data obtained with both the servo and analyzing cavities stabilized to the  $3.39\ \mu\text{m}$  local oscillator. At longer averaging times ( $\tau > 10\ \text{sec}$ ), curve A is dropping rapidly and should ultimately approach the stability of the methane-stabilized He-Ne laser ( $\sigma = 1 \times 10^{-13}$ ). Curve B represents data obtained without cavity length stabilization. The dashed portion for  $\tau > 0.1\ \text{sec}$  shows the estimated loss of stability due to cavity temperature drifts and strain instabilities in the cavity PZT crystals.

The maximum in curve A near  $\tau = 1\ \text{sec}$  results from noise in the  $3.39\ \mu\text{m}$  fringe amplifiers being mapped into cavity length instability, and therefore, into dye laser frequency instability. This would be removed by better  $3.39\ \mu\text{m}$  frequency discrimination.

Curve C shows the equivalent frequency noise of the servo loop error signal. This represents the best stability which could be achieved with this servo system.

### Laser Saturation of Atomic Beams

Although the long term frequency stability of the dye laser is quite good, the resetability and accuracy are not nearly as satisfactory. In principle, this limitation can be overcome by locking the dye laser to a very narrow atomic transition. A possible way of doing this, using a magnetically deflected beam of calcium atoms, is discussed below.

### Saturation Spectroscopy of Calcium

An experiment to observe the  $1S_0 - 3P_1$  intercombination transition in calcium under high resolution conditions uses the apparatus depicted schematically in Fig. 3. The properties of this transition which make it suitable for use as a possible frequency/wavelength standard in the visible region of the spectrum are listed in Table 1. In Fig. 3, a heated oven is used to produce a beam of Ca atoms in the  $1S_0$  ground state. The radiation from the stabilized dye laser, after passing through the appropriate isolators and beam expanding optics, enters the calcium atomic beam apparatus where it crosses the calcium atomic beam at approximately

right angles. A mirror, placed at the far side of the apparatus, reflects the laser beam back onto itself. Under the proper conditions, in the region where the two beams cross, the  $^1S_0$  calcium atoms can be excited to the  $^3P_1$  state. The transition can be observed by magnetically deflecting the excited  $^3P_1$  atoms and then detecting these same atoms using an off-axis hot wire detector. The advantages of using calcium are:

- (1)  $^{40}\text{Ca}$  is 99.7% naturally abundant.
- (2)  $^{40}\text{Ca}$  has zero nuclear spin, and therefore exhibits no hyperfine structure.
- (3) The  $^1S_0$  ground state is non-degenerate so that the entire atomic beam is in a single ground state.
- (4) The  $^1S_0 - ^3P_1$  transition occurs at a wavelength ( $\lambda_{\text{air}}$  = 6573 Å) where the stabilized dye laser can deliver the required power ( $\approx 5\text{mW}$ ).
- (5) The  $^3P_1$  natural lifetime<sup>5</sup> of 0.39 ms is sufficiently long to ensure, ultimately, a very narrow linewidth (410 Hz) for the optical transition. The lifetime is also long enough to allow atoms in the  $^3P_1$  state to be magnetically deflected before decaying to the  $^1S_0$  state.
- (6) The  $^1S_0$  ground state is diamagnetic only, and is therefore virtually undeflected by an inhomogeneous magnetic field.
- (7) The  $^3P_1$  state is paramagnetic and has  $g_J = 1.5$ . The very large magnetic moment which results, permits easy deflection of the  $^3P_1$  state in an inhomogeneous magnetic field.
- (8) The hot wire detection efficiency<sup>6</sup> for ground state calcium atoms (using an oxygenated tungsten wire) is of the order of 1 to 10%.

Some of these properties (including those given in Table 1), and their advantages for a proposed frequency standard using fine structure transitions in a magnesium or calcium beam, have been pointed out by Strumia.<sup>7</sup> A general discussion of the proposed use of saturated absorption for the 6573 Å calcium atomic beam transition has also been given by Hall and Snyder.<sup>8</sup>

Experiments conducted so far have concentrated on testing the detection system. In these experiments, metastable calcium atoms in the  $^3P_2$ ,  $^3P_1$ , and  $^3P_0$  states were produced by bombarding the 0.05 cm diameter oven hole with electrons and thus producing a plasma discharge in the oven hole. This method, which is due to Brink,<sup>9</sup> yields up to  $\sim 5\%$   $^3P_2$  and  $^3P_1$  atoms. Initially, it was hoped that  $^3P_1$  calcium might exhibit a higher hot wire detection efficiency than  $^1S_0$  calcium, which would have obviated the need for magnetic deflection, but the effect appears to be small, if it exists at all. Using the flop-out detection scheme shown in Fig. 3, we have achieved signal-to-noise detection ratios

for  $^3P_2$  atoms of up to 50:1 with  $\sim 2\frac{1}{2}\%$  of the atomic beam in the  $^3P_2$  state. (We were not able to assess the detection method directly for  $^3P_1$  because the oven is many decay lengths from the deflecting magnet. We were able to use  $^3P_2$  atoms, however, because of their much longer lifetime. It is expected that the results for  $^3P_1$  atoms would be the same.) Note that, if the hot wire detection efficiencies for  $^1S_0$  and  $^3P_1$  calcium are essentially the same,  $^3P_1$  atoms which decay after passing through the magnet, but before reaching the hot wire, will still be detected.

The mirror in Fig. 3, which reflects the laser beam back onto itself, should allow us to perform saturation spectroscopy on the calcium beam. Since the Doppler width of our beam is  $\sim 175$  kHz, whereas the ultimate natural linewidth of the  $^1S_0 - ^3P_1$  transition is  $\sim 400$  Hz, the saturated absorption technique is essential for obtaining a narrow line.

In the initial experiments using the laser, the linewidth will be determined by the time-of-flight (TOF) of the atoms through the laser beam (i.e., by the diameter for a circular cross section laser beam). Also, it is necessary to provide magnetic shielding in the interaction region since the transition will be to the magnetically sensitive  $m_J = \pm 1$  Zeeman sublevels of the  $^3P_1$  state. Later experiments will induce the transition to the  $m_J = 0$  Zeeman sublevel instead, which has the advantage of being very insensitive to magnetic fields. To magnetically detect this transition, it will be necessary to induce a  $\Delta m_J = \pm 1$  RF Zeeman transition in the excited state subsequent to laser excitation.

The use of an atomic beam rather than an absorption cell has at least one advantage for very high resolution work. In an absorption cell, the TOF of the atoms across the laser beam must be uninterrupted if the best resolution is to be realized. This requires that the atomic mean free path be greater than the diameter of the laser beam. Because of the resultant low density of atoms, it is necessary to use a very long absorption cell (of the order of 10 meters, or greater) if the absorption signal is to be observable. The atomic beam method has the advantage that the saturation signal is observed directly, rather than as a small change in a large background. Consequently, the amount of absorption need not be large, and a relatively short apparatus can be used.

The initial experiments on calcium will be designed to provide a demonstration of the technique of atomic beam saturation spectroscopy. If the TOF linewidth and broadening due to magnetic field inhomogeneities can be kept small enough, it should be possible to observe (and eventually, completely resolve) the 23 kHz relativistic recoil splitting<sup>10</sup> of the calcium line.

#### Advantages of Calcium as a Possible $\nu/\lambda$ Standard

Based on the properties of the  $^1S_0 - ^3P_1$  Ca transition, as given in Table 1, the ultimate projected frequency and wavelength stability of a laser-excited calcium beam device is  $\lesssim 10^{-15}$ . The main disadvantage of such a device as a possible frequency/wavelength standard in the visible region of the spectrum is presumably only a temporary

disadvantage: At the present time, there is no way to measure the frequency of the Ca transition in terms of the Cs hyperfine frequency. The extension of frequency measurements into the IR and visible continues,<sup>11</sup> however, and further progress in this area can be expected in the future.

Measurement of the Rydberg Constant

In addition to the calcium beam experiment, we are working on an experiment which will determine the Rydberg constant with improved accuracy. In this experiment, a beam of metastable H atoms ( $2^2S_{1/2}$ ) is generated by electron bombardment of ground state H atoms produced in an RF discharge. Metastable atoms in the beam are detected by applying an electric quenching field and observing the resulting Lyman  $\alpha$  photons. Laser saturation of the Balmer  $\alpha$  transition ( $\lambda = 6563 \text{ \AA}$ ) results in a decrease in the observed Lyman  $\alpha$  signal.

By using an atomic beam rather than a discharge, perturbations such as Stark shifts and collisional effects should be virtually eliminated. The lifetime-limited linewidth of the Balmer  $\alpha$  transition is about 30 MHz;<sup>12</sup> however, by simultaneously applying an RF field<sup>12</sup> at the frequency corresponding to the  $3^2P_{1/2} - 3^2S_{1/2}$  transition, the linewidth can be reduced to  $\approx 1$  MHz. By using the interferometer previously used to make the wavelength measurement<sup>13</sup> of the methane-stabilized He-Ne laser ( $\lambda = 3.39 \text{ \mu m}$ ), the Balmer  $\alpha$  wavelength can be measured to a few parts in  $10^{10}$ . The resulting accuracy in the Rydberg should be less than one part in  $10^9$ .

REFERENCES

1. R. L. Barger, M. S. Sorem, and J. L. Hall, Appl. Phys. Lett. 22, 573 (1973).
2. F. Y. Wu, R. E. Grove, and S. Ezekiel, Appl. Phys. Lett. 25, 73 (1974).
3. R. L. Barger, J. B. West, and T. C. English, Appl. Phys. Lett. 27, 31 (1975).
4. R. L. Barger and J. L. Hall, Phys. Rev. Lett. 22, 4 (1969).
5. J. J. Wright, P. S. Turciniti, and L. C. Balling, Fourth International Conference on Atomic Physics, Heidelberg, July 22-26, 1974 Abstracts of Contributed Papers, p.200.
6. R. Müller and H.-W. Wassmuth, Surf. Sci. 40, 15 (1973).
7. F. Strumia, Metrologia 8, 85 (1972).
8. J. L. Hall and J. J. Snyder, "Prognosis for Optical Frequency Standards Using Forbidden Atomic Transitions," submitted for publication, 1975.
9. See for example, G. O. Brink and R. J. Hull, Phys. Rev. 179, 43 (1969). We thank G. Brink for helpful discussions and advice on production of metastables.

10. Ch. Bordé and J. L. Hall in Laser Spectroscopy, Plenum Press, 1974, p. 125.
11. K. M. Evenson and F. R. Petersen in Physics of Quantum Electronics, Vol. 2, Laser Applications to Optics and Spectroscopy, Addison-Wesley, 1975, p. 367. The highest frequency measured to date (148 THz) is described in, D. A. Jennings, F. R. Petersen, and K. M. Evenson, Appl. Phys. Lett. 26, 510 (1975).
12. D. E. Roberts and E. N. Fortson, Phys. Rev. Lett. 31, 1539 (1973).
13. R. L. Barger and J. L. Hall, Appl. Phys. Lett. 22, 196 (1973).

TABLE I  
PROPERTIES OF THE CALCIUM  $^1S_0 - ^3P_1$  TRANSITION AS A POSSIBLE FREQUENCY/WAVELENGTH STANDARD IN THE VISIBLE

Bohr frequency	455.986 33 THz	
Lifetime of $^3P_1$	$(\lambda_{vac} \approx 6574.593 \text{ 0 \AA})$ 0.39 ns	
Ultimate natural linewidth (FWHM)	410 Hz	
Lifetime - limited Q	$1 \times 10^{12}$	
Recoil splitting	23 kHz	
First - order Doppler shift	none (saturation spectroscopy)	
Second - order Doppler shift	-1.7 kHz	$[-5 \times 10^{-15}/\text{C}]$
Zeeman effect	$\sim 1 \text{ Hz/G}^2$	$[2 \times 10^{-15}/\text{G}^2]$
Stark effect	$\lesssim 1 \text{ Hz}/(\text{V/cm})^2$	$[2 \times 10^{-15}/(\text{V/cm})^2]$
Optimum laser power	$\approx 5 \text{ mW}$	
Intensity dependent frequency shift	none (recoil doublet resolved)	

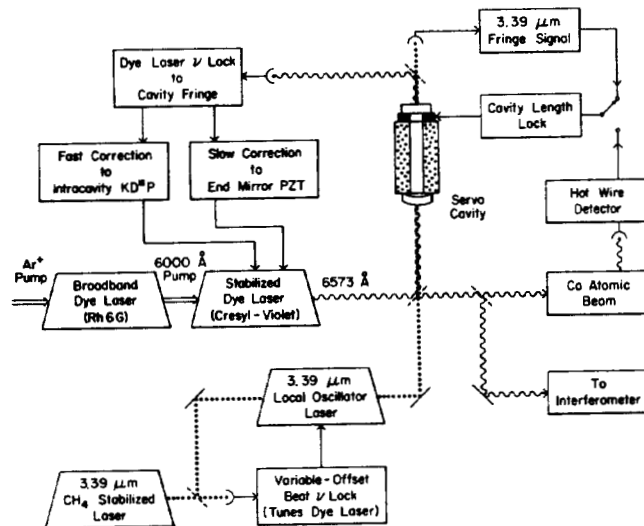


Figure 1. Block diagram of dye laser stabilization scheme.

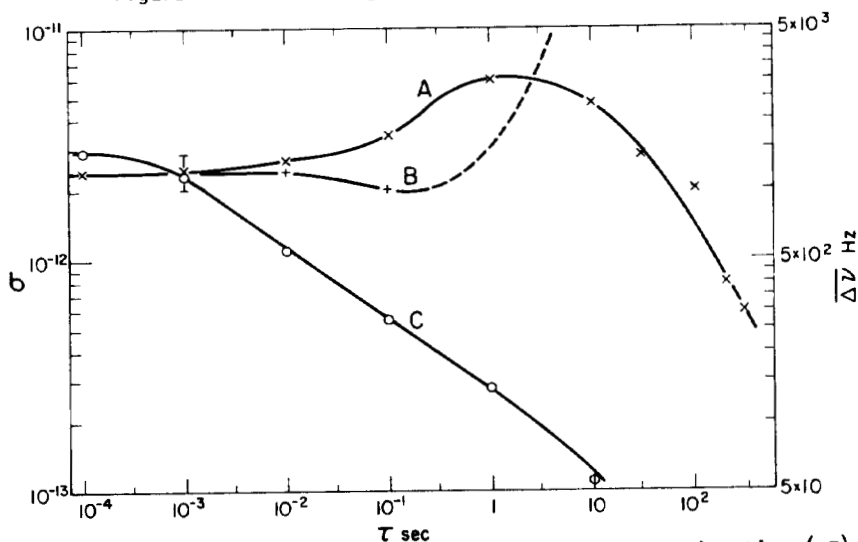


Figure 2. Plot of Allan variance ( $\sigma$ ) versus averaging time ( $\tau$ ) for stabilized dye laser.

SATURATION SPECTROSCOPY OF CALCIUM

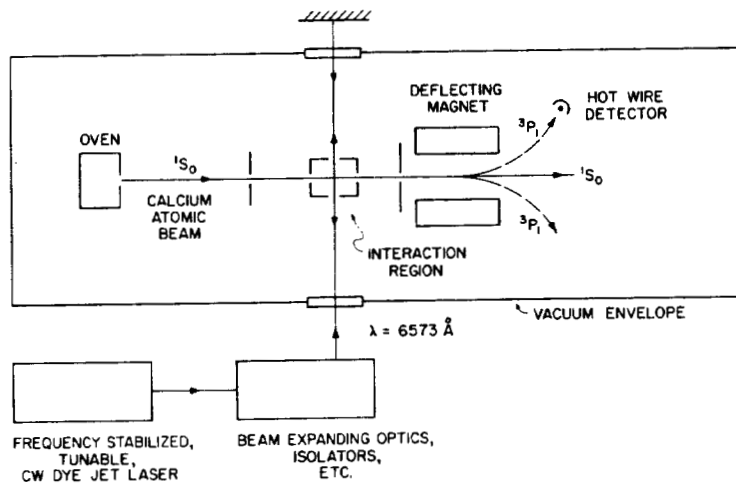


Figure 3. Schematic diagram of atomic calcium beam and detection system.